Structures of ultrathin copper nanotubes



2002 J. Phys.: Condens. Matter 14 8997

(http://iopscience.iop.org/0953-8984/14/39/309)

INSTITUTE OF PHYSICS PUBLISHING JOURNAL OF PHYSICS: CONDENSED MATTER

J. Phys.: Condens. Matter **14** (2002) 8997–9005 PII: S0953-8984(02)39538-9

# Structures of ultrathin copper nanotubes

**Jeong Won Kang, Jae Jeong Seo and Ho Jung Hwang**

Institute of Technology and Science, Semiconductor Process and Device Laboratory, Department of Electronic Engineering, Chung-Ang University, 221 HukSuk-Dong, DongJak-Ku, Seoul 156-756, Korea

E-mail: gardenriver@korea.com

Received 16 July 2002, in final form 19 August 2002
Published 19 September 2002
Online at stacks.iop.org/JPhysCM/14/8997

**Abstract**

We have performed atomistic simulations for helical multi-shell (HMS) Cu nanowires and nanotubes. Our investigation on HMS Cu nanowires and nanotubes has revealed some physical properties that were not dealt with in previous works that considered metal nanowires. As the diameter of HMS nanowires increases, their cohesive energy per atom decreases but their optimal lattice constants are almost constant. Shell–shell or core–shell interactions mainly affect the lattice constant and the diameter of HMS nanowires or nanotubes. Our molecular dynamics simulations show that parts of ultrathin Cu nanotubes collapse into the empty core at low temperature and this is the main mechanism for the transformation from ultrathin nanotube to nanowire structures. This study shows that HMS Cu nanotubes can retain their own structures when the internal stresses on HMS nanotubes are zero or towards the outside.

(Some figures in this article are in colour only in the electronic version)

## 1. Introduction

Recently, ultrathin metal nanowires have aroused growing interest in condensed matter physics; for example, Takayanagi's group has fabricated ultrathin gold [1–3] and platinum [4] nanowires. Many theoretical studies on ultrathin nanowires have been made using atomistic simulations for several metals, and these have simulated straight uniform ultrathin nanowires containing helical multi-shell (HMS) structures made of metals such as Ag [5], Al [6], Au [7–10], Ti [11], Cu [12, 13], and Zr [14]. Unlike the hexagonal network of carbon nanotubes, each shell of the HMS structures is formed by a triangular network which is similar to the $\{111\}$ atomic sheet of fcc crystals. The $\langle 110 \rangle$ atomic rows in each $\{111\}$ sheet make a helix that coils around the axis of the metal nanowires. The $n$–$n'$–$n''$–$n'''$ HMS nanowires, then, are composed of coaxial tubes with $n$, $n'$, $n''$, $n'''$ helical atom rows ($n > n' > n'' > n'''$).

  

**Table 1.** For structures of HMS Cu nanowires and nanotubes, the number of atoms in the supercell, the optimal lattice constant along the wire axis ($a$), the cohesive energy per atom ($E_{coh}$), and the mean diameter of the shell composed of six atoms ($D_{6s}$).

| Structure | Number of atoms in supercell | $a$ (Å) | $E_{coh}$ (eV) | $D_{6s}$ (Å) |
|---|---|---|---|---|
| 5–1 nanowire | 180 | 2.2500 | −2.903 27 | — |
| 10–5–1 nanowire | 480 | 2.2500 | −3.097 03 | — |
| 15–10–5–1 nanowire | 930 | 2.2563 | −3.206 78 | — |
| 6–1 nanowire | 210 | 2.2435 | −2.942 16 | 4.788 440 |
| 11–6–1 nanowire | 540 | 2.2396 | −3.152 02 | 4.734 468 |
| 16–11–6–1 nanowire | 1020 | 2.2386 | −3.244 11 | 4.691 218 |
| 6–0 nanotube | 180 | 2.0913 | −2.586 86 | 5.012 518 |
| 13–6 nanotube | 570 | 2.2184 | −2.988 25 | 5.405 746 |
| 16–10 nanotube | 720 | 2.2185 | −3.059 57 | — |

In addition to studies on novel helical structures of ultrathin nanowires, investigations of the melting behaviour of ultrathin nanowires of Pb [15], Au [16], Cu [17], and Ti [18] have been carried out. Compression of the HMS Au nanowires [19] and tensile testing of the HMS Cu nanowires [20] have also been performed using classical molecular dynamics (MD) simulations. The resonance of ultrathin Cu nanobridges was investigated using a classical MD simulation [21]. In a study on defects in the HMS Cu nanowires [22], the vacancy formation energy was lowest in the core of a HMS-type nanowire, vacancies formed in the outer shell of a HMS-type nanowire naturally migrated toward the core, and an onion-like cluster with a hollow was also formed. These results provided basic information on the formation of hollow HMS-type metal nanowires. Recently evidence of suspended 13–6 HMS Pt nanotubes was reported from experiments [4] and Bilalbegovic also compared the structure of the 16–10 Au nanotube with double-wall carbon nanotubes in a classical MD simulation.

Although the previous works have supported the assertion that metal nanowires have HMS structures, further investigations, in areas such as non-linear ultrathin nanowires, funnel-shaped nanowires, defects in nanowires, and metal tubular structures such as carbon nanotubes need to be made in order to understand the physical properties of nanowires, and for the successful application of nanowires in nanoscale devices. Therefore, this investigation focuses on copper HMS nanotubes and provides basic physical information on the structural properties of HMS-type nanotubes.

## 2. Computational methods

For the Cu–Cu interactions, we used a well fitted many-body potential function in the second-moment approximation of the tight-binding (SMA-TB) scheme [24]. This potential function reproduces many basic properties of crystalline and non-crystalline bulk phases and surfaces [25], and provides good insight into the structure and thermodynamics of metal clusters [26, 27]. Table 1 (also given in [28]) shows that the physical values of Cu calculated by the SMA-TB method agree with values obtained by other theoretical methods, and also with those measured by experiment. The SMA-TB potential has previously been used in atomic-scale simulation studies of nanoclusters [29–32] and nanowires [28, 33–38]. We used the same values for the parameters for the SMA-TB method as are given in [24]. The cut-off distance, 5.30 Å, is the average distance between the fourth-and fifth-nearest neighbours in a perfect crystal.

The optimal atomic arrangements were obtained using the steepest descent (SD) method, which is the simplest of the gradient methods, and this was called the gradient descent

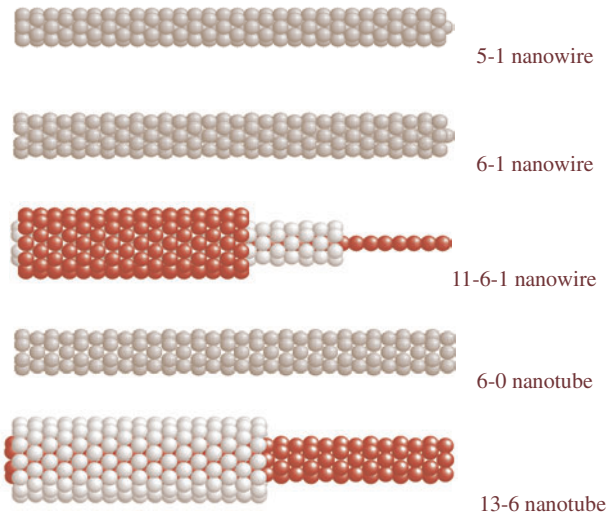


**Figure 1.** Structures of well defined ultrathin copper nanowires and nanotubes obtained from the SD simulations at $T = 0$ K.

method. The choice of direction was determined by where the force exerted by the interatomic interaction decreased the fastest, which was in the opposite direction to $\nabla E_i$. In this work, the SD method was applied to the atomic positions, and the next atomic position vector ($\boldsymbol{r}_i'$) was obtained by a small displacement of the existing atomic position vector ($\boldsymbol{r}_i$) along a chosen direction under the condition $|\boldsymbol{r}_i' - \boldsymbol{r}_i|/|\nabla E_i| = 0.001$.

The structures of ultrathin metal nanowires found using the embedded atom model (EAM) potential [6, 8–10, 16, 19] are the same as those found using the SMA-TB potential [7, 11, 12, 14, 18]. These results have been found for the structures [6, 7, 10–12], the cohesive energies per atom as a function of diameter [6, 34], bond angle distributions [6, 11, 12], and melting properties [15, 36] of nanowires. Table 1 shows all the structures that are investigated in this paper and figure 1 shows a 5–1, a 6–1, and an 11–6–1 HMS Cu nanowire and a 6–0 and a 13–6 HMS Cu nanotube. We selected the series of 5–1 and 6–1 HMS nanowires investigated in previous works [12, 14], 6–0 and 13–6 nanotubes found in experiments [4], and the 16–10 nanotube found in a MD simulation [23]. Circular folding of the $\{111\}$ sheet made each shell of the HMS nanowires and nanotubes. The HMS nanowires and nanotubes were relaxed using the SD method. While the cores of the HMS nanowires are filled with atomic strands, the cores of the HMS nanotubes are empty. Each shell is composed of thirty atomic layers along the wire axis, and a periodic boundary condition (PBC) is applied to supercells of nanowires and nanotubes. To provide for easy appreciation of the structures of the HMS nanowires and nanotubes, figure 1 shows the stripped structures of the 11–6–1 HMS nanowire and the 13–6 HMS nanotube. Table 1 shows the numbers of atoms in supercells. The optimal lengths of PBCs for nanowires and nanotubes are related to their diameters, and this will be considered in relation to table 1 and figure 2 in the next section.

## 3. Results and discussion

Table 1 shows the optimal lattice constants, the cohesive energies per atom, and the mean diameters of the shell composed of six atoms for the optimal structures of nanowires and

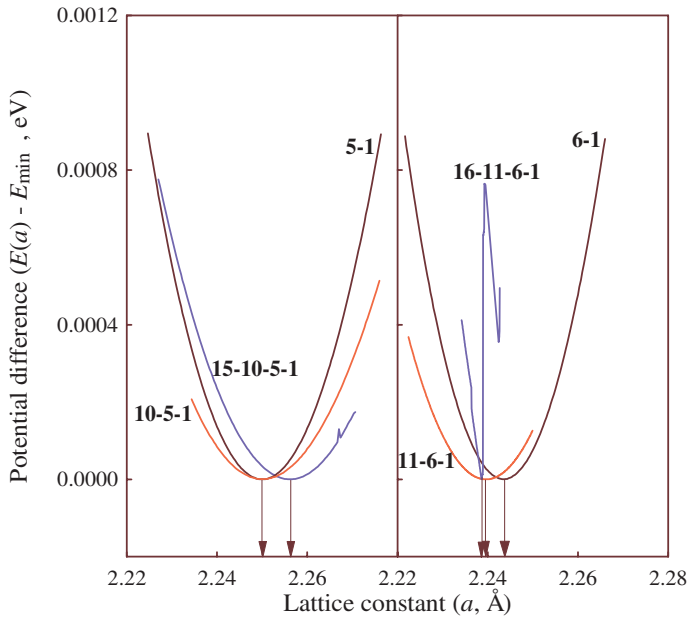


**Figure 2.** Total cohesive energy as a function of lattice constant for 5–1, 6–1, and 11–6–1 HMS Cu nanowires.

nanotubes based on the SMA-TB potential. We calculated optimal lattice constants of nanowires and nanotubes along the wire axis as follows: using the structures of table 1, as the lattice constants ($a$) of those increased by 0.0001 from 2.22 Å, the optimal structure of each step was obtained by the SD method and then the cohesive energies per atom ($E(a)$) were calculated. The points at the lowest cohesive energy ($E_{min}$) are the optimal lattice constants that are shown in table 1, and figure 2 shows the potential differences ($E(a) - E_{min}$) as a function of lattice constant for the 5–1, 10–5–1, 15–10–5–1, 6–1, 11–6–1, and 16–11–6–1 HMS Cu nanowires. The optimal lattice constant of the 15–10–5–1 HMS nanowire is 0.0063 Å higher than those of the 5–1 and 10–5–1 HMS nanowires, 2.25 Å. For the 6–1 HMS series, as the diameter increases, the optimal lattice constant slightly decreases. However, since the differences between the optimal lattice constants of HMS nanowires are within 0.0177 Å, the optimal lattice constants of HMS nanowires are almost constant irrespective of the diameter of the HMS nanowires. As the lattice constant increases, some sharp curves of the cohesive energy for the 16–11–6–1 HMS nanowire are shown, since its diameter increases more or decreases less.

We also calculated the optimal lattice constants of nanotubes by using the same procedure, and the results obtained are shown in table 1. The optimal lattice constant of the 6–0 nanotube is much smaller than those of the HMS nanowires. However, in the case of the 13–6 and 16–10 HMS nanotubes, the lattice constant is higher than that of the 6–0 nanotube because of the interaction between the inner and outer shells, and is similar to those of the HMS nanowires (within 1.4%). Therefore, from this result it appears that the shell–shell or core–shell interactions mainly affect the lattice constants of the HMS nanowires or nanotubes. For the HMS nanowires, since their cores are filled with linear atomic strands and their shells are made by circular folding of {111} sheets, both the distance between atoms in the core and the height of the triangles in the outer shell are mainly related to the lattice constants of the HMS nanowires. However, since the HMS nanotubes are only made by circular folding of {111} sheets, the height of the triangles is only related to the lattice constants of the HMS

nanotubes. In table 1, the lattice constant of the 6–0 nanotube is 93.33% of that of the 6–1 nanowire. In the case of the 6–0 nanotube, when the length of a side of a normal triangle is 1, the height of the triangle is $\sqrt{3}/2 = 0.866$. In the case of the 6–1 nanowire, when both the length of a side of a normal triangle and the distance between atoms in the core strand are 1, the average of the height of a triangle, $\sqrt{3}/2$, and the distance between atoms in the core strand, 1, is $(2 + \sqrt{3})/4 = 0.933$. Therefore, the lattice constant of the 6–0 nanotube is 92.82% of that of the 6–1 nanowire, from the above two values. This value, 92.82%, is in good agreement with that (93.33%) obtained from our simulation. From these results, since the 6–1 nanowire has atomic strands as the core, the lattice constants and the diameters of the 6–1 nanowire are different with those of the 6–0 nanotube. In the case of a double-shell nanotube, the 13–6 nanotube, the interaction between the inner and outer shells also leads to a larger lattice constant than for a single-shell nanotube.

In previous works, the cohesive energies per atom ($E_{coh}$) for nanowires have been taken as linearly proportional to the reciprocal of the diameter ($D$) [6, 33], and are expressed as follows:

$$E_{coh} \approx E_{bulk} + n/D, \tag{3.1}$$

where $E_{bulk}$ is the cohesive energy of the atoms of the bulk material and $n$ is a constant. As the number of shells in the HMS nanowires increases, their cohesive energy per atom increases and the relation of equation (3.1) has been demonstrated in our previous work [33]. In this investigation, since we considered only the 6–0, 13–6, and 16–10 HMS nanotubes, this work could not provide a relationship between $E_{coh}$ and $D$ for the HMS nanotubes. However, our results show that the values of $E_{coh}$ for the 13–6 and 16–10 HMS nanotubes with double shells are lower than that of the 6–0 nanotube with a single shell.

While the number of atoms in the 5–1 nanowire is equal to that in the 6–0 nanotube, since $E_{coh}$ for the 5–1 nanowire is lower than $E_{coh}$ for the 6–0 nanotube, this means that the 5–1 nanowire is more stable than the 6–0 nanotube from a potential energy point of view. Our classical MD simulations of the 6–0 nanotube showed that the 6–0 nanotube was transformed into a nanowire with complex structures including the structure of a 5–1 nanowire, and this will be discussed below. For the 16–10 Cu nanotube, the value of the potential energy per atom obtained is 0.4844 eV/atom higher than that for the Cu bulk, −3.544 eV/atom. If we consider the cohesive energy for the Cu bulk material, the cohesive energy for the 16–10 Cu nanowire is only 86.33% of that of the bulk. The cohesive energy per atom for the 16–11–6–1 nanowire is 0.2999 eV/atom higher than that for the bulk material and is 91.54% of that of the bulk. Therefore, one can see that the Cu nanotubes studied are more unstable structures than the HMS Cu nanowires from the potential energy point of view. When the number of atoms composing a nanowire is the same as the number composing a nanotube, since the cohesive energy per atom for the nanowire is much lower than that for the nanotube, it is very difficult to obtain tube-like structures from a simulated annealing method.

We calculated the mean diameter ($D_{6s}$) of the shell composed of six atoms for the 6–1 and 11–6–1 HMS nanowires and the 6–0 and 13–6 HMS nanotubes. In the case of the 11–6–1 HMS nanowire, since the outer shell slightly compresses the inner shell, $D_{6s}$ for the 11–6–1 HMS nanowire is slightly smaller than $D_{6s}$ for the 6–1 nanowire. $D_{6s}$ for the HMS nanotubes is larger than $D_{6s}$ for the HMS nanowires. While the lattice constant of the 6–1 nanowire is larger than that of the 6–0 nanotube, $D_{6s}$ for the 6–1 nanowire is smaller than $D_{6s}$ for the 6–0 nanotube. Therefore, the difference between the volumes of the 6–1 nanowire and the 6–0 nanotube is 2.296%, and this result implies that a 6–0 nanotube has a different geometry of the shell composed of six atoms under conditions of constant volume. In this work, the distance between shells of the nanotubes is 2.165 Å.

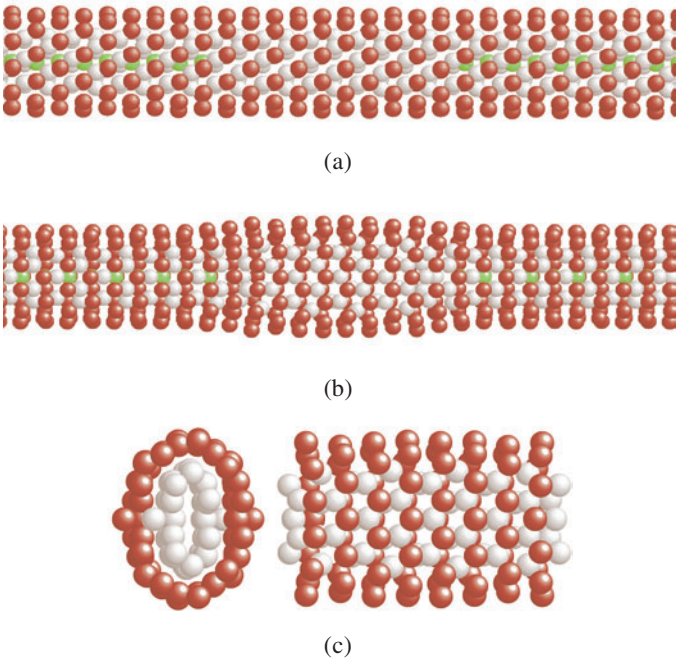

**Figure 3.** (a) The initial structure of an 11–6–1 HMS Cu nanowire with a hollow, (b) the structure relaxed by the SD method, and (c) side and cross-sectional views of the region without an atomic strand in the core in (b).

In previous work [22], as the diameter of the HMS nanowire increased, the vacancy formation energy of its core decreased rapidly. MD simulations also showed that vacancies migrated from the outer shell to the inner shell and to the core. Since the formation energy of a vacancy was lowest at the core and the vacancy migrated towards the lower-energy states, the vacancy migrated to the core. Therefore, these results implied that vacancies would be most frequently found in the core of a HMS nanowire. This interpretation is in good agreement with previous results that showed evidence of metal nanotubes and high-resolution transmission electron microscopy (HRTEM) images of 6–0 and 13–6 HMS Pt nanotubes. Therefore, we investigated an 11–6–1 HMS nanowire with a hollow region as shown in figure 3(a). Some core atoms in the centre region of the 11–6–1 HMS nanowire were omitted and then this structure, figure 3(a), was relaxed by the SD method and transformed into the structure shown in figure 3(b). The region with a hollow of the 11–6–1 HMS nanowire disappeared due to the pressure on the inner shell, 20.663 GPa, as shown in figure 3(b). Figure 3(c) shows side and cross-sectional views of a region without an atomic strand in the core. These results show that the hollow region disappears because the forces exerted on the atoms of the inner or outer shell acted towards the core. By analogy with this result, when the pressures acting on the inner shell of a HMS nanotube are zero or very low, the nanotube will be a stable structure. This interpretation is also related to the mean diameter ($D_{6s}$) of the shell composed of six atoms. As shown in table 1, $D_{6s}$ for nanotubes is larger than $D_{6s}$ for nanowires. In particular, the $D_{6s}$-values for the 13–6 Cu HMS nanotube are the largest found in this work, and this is because the interaction between the inner and outer shells is attractive. The Takayanagi group also showed a HRTEM image of a 13–6 Pt HMS nanotube obtained from a suspended nanowire made by an electron-beam thinning method [4].

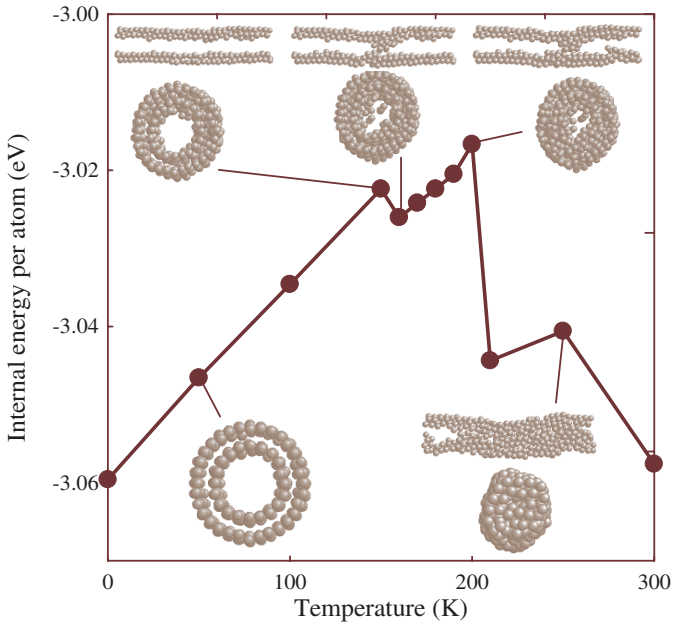


**Figure 4.** Internal energy per atom as a function of temperature for the 16–10 Cu nanotube and cross-sectional side views of the 16–10 nanotube at 150, 160, 200, and 250 K, respectively.

We also investigated the curve of the internal energy per atom for the 16–10 Cu nanotube. The Cu nanotube was heated up in steps via scaling the atomic velocities with zero total linear and angular momenta. On heating, temperature was increased from 0 in 50 K intervals, but it was changed in steps of 10 K near the structural transition temperatures. At each temperature, MD runs of $2 \times 10^5$ steps were carried out with a time step of 0.5 fs (total 100 ps). The mean kinetic temperature $k_B T = [2/(3N - 6)]\langle\sum_{i=1}^{N} (mv_i^2/2)\rangle$, where the angular brackets denote averaging over time and $k_B$ is the Boltzmann constant, supplying the energy to atoms in the nanotube, and the internal energy curve of the nanotubes with this kinetic temperature, as shown in figure 4, were obtained from the last $10^3$ steps. A code based on a constant-temperature MD scheme was used to carry out all simulations in this paper and in previous works [13, 17, 22].

Figure 4 shows the internal energy per atom as a function of temperature and also includes some atomic structures to show the structural transition of the 16–10 Cu nanotube. Below 150 K, the 16–10 nanotube maintained a tubule structure. From 160 to 200 K, parts of the nanotubes collapsed to block the tube, but most of the nanotube had hollow regions as shown in figure 4. When a nanotube caved in, a slight downward curvature of the internal energy curve occurred, at the 160 K point in figure 4. Above 200 K, the curve rapidly decreased and the 16–10 Cu nanotube was transformed into a Cu nanowire because the structure of the nanotube collapsed; then the hollow region rapidly decreased and the hollow region of the nanowire disappeared at 300 K. In the previous MD simulation work [23] for a 16–10 Au nanotube based on a glue model potential [39], Bilalbegovic showed the high-temperature stability of the 16–10 Au nanotube, and showed that several atoms evaporated into the empty core at 900 K. Both studies show the degradation of the inner shell toward the empty core, and Bilalbegovic's results are similar to ours except that several atoms evaporated into the empty core at a high temperature; our results show that atoms in the inner shell of the 16–10 Cu

nanotube did not evaporate into the empty core at high temperature but parts of the 16–10 Cu nanotube collapsed into the empty core at low temperatures. It seems that this difference may be due to both the differences in the materials and in the empirical potentials used. While the glue model potential [39] used in Bilalbegovic's work considers only the interactions between first neighbours, the SMA-TB potential used in this work covers the long-range interactions which are important in metallic materials. A more detailed study needs to be made in future work. We also performed MD simulations for the 6–0 Cu nanotube at very low temperatures. Since the cut-off distance, 5.30 Å, for the SMA-TB potential is longer than the diameter of the 6–0 Cu nanotube, the 6–0 Cu nanotube was crushed and transformed into a nanowire in the case of MD simulations at just 30 K. For carbon material, since a single graphite sheet is a stable structure, a single-shell carbon nanotube is also stable. However, for copper material, since a single $\{111\}$ sheet is an unstable structure, a single-shell Cu nanotube is also unstable. The cohesive energy per atom for a Cu$\{111\}$ sheet is $-2.523$ eV, which is higher than that for the 6–0 Cu nanotube. Though HMS Cu nanotubes are more stable than a Cu$\{111\}$ sheet, our MD simulation results show that the structures of ultrathin Cu nanotubes are unstable and limited to very low temperatures, since the potential energies of Cu nanotubes are much higher than those of Cu nanowires.

## 4. Conclusions

This study on HMS Cu nanowires and nanotubes has revealed some physical properties that were not dealt with in previous works that considered metal nanowires. As the diameter of nanowires increases, their cohesive energy per atom decreases but their optimal lattice constants are almost constant. Shell–shell or core–shell interactions mainly affect the lattice constant and diameter of the HMS nanowires or nanotubes. Simulation results for an 11–6–1 HMS nanowire with a hollow region showed that the region with the hollow disappeared because of the pressure acting on the inner shell. Cu nanotubes were unstable structures from the potential energy point of view and MD simulations showed that the structures of Cu nanotubes were limited to very low temperatures. Our MD simulations also showed that parts of ultrathin Cu nanotubes collapsed into the empty core at low temperature and this is the main mechanism for the transformation from ultrathin nanotube to nanowire. From this study, we conclude as follows: for copper material, when the internal stresses on HMS nanotubes are zero or toward the outside, the HMS nanotubes can be maintained only at low temperatures.

## References

[1] Kondo Y and Takayanagi K 1997 *Phys. Rev. Lett.* **79** 3455
[2] Ohnishi H, Kondo Y and Takayanagi K 1998 *Nature* **395** 780
[3] Kondo Y and Takayanagi K 2002 *Science* **289** 606
[4] Oshima Y, Koizumi H, Mouri K, Jirayama H and Takayanagi K 2002 *Phys. Rev.* B **65** 121401
[5] Finbow G M, Lynden-Bell R M and McDonald I R 1997 *Mol. Phys.* **92** 705
[6] Gülseren O, Ercolessi F and Tosatti E 1998 *Phys. Rev. Lett.* **80** 3775
[7] Wang B, Yin S, Wang G, Buldum A and Zhao J 2001 *Phys. Rev. Lett.* **86** 2046
[8] Tosatti E, Prestipino S, Kostlmeier S, Dal Corso A and Di Tolla F D 2001 *Science* **291** 288
[9] Bilalbegovic G 1998 *Phys. Rev.* B **58** 15 412
[10] Bilalbegovic G 2000 *Comput. Mater. Sci.* **18** 333
[11] Wang B, Yin S, Wang G and Zhao J 2001 *J. Phys.: Condens. Matter* **13** L403
[12] Hwang H J and Kang J W 2002 *J. Korean Phys. Soc.* **40** 283
[13] Kang J W and Hwang H J 2002 *J. Phys.: Condens. Matter* **14** 2629
[14] Wang B, Wang G and Zhao J 2002 *Phys. Rev.* B **65** 235406
[15] Gülseren O, Ercolessi F and Tosatti E 1995 *Phys. Rev.* B **51** 7377

[16] Bilalbegovic G 2000 *Solid State Commun.* **115** 73
[17] Kang J W and Hwang H J 2002 *J. Korean Phys. Soc.* **40** 946
[18] Wang B, Wang G and Zhao J 2002 *Preprint* cond-mat/0202522
[19] Bilalbegovic G 2001 *J. Phys.: Condens. Matter* **13** 11 531
[20] Kim W W, Kang J W, Kim T W, Hwang H J and Lee G Y 2002 *J. Korean Phys. Soc.* **40** 889
[21] Kang J W and Hwang H J 2002 *Nanotechnology* **13** 503
[22] Kang J W, Seo J J, Byun K R and Hwang H J 2002 *Phys. Rev.* B **66** 125405
Kang J W, Seo J J, Byun K R and Hwang H J 2002 *Preprint* cond-mat/02007119
[23] Bilalbegovic G 2002 *Preprint* cond-mat/0206504
[24] Cleri F and Rosato V 1993 *Phys. Rev.* B **48** 22
[25] Guillopé M and Legrand B 1989 *Surf. Sci.* **215** 577
[26] Lee Y J, Maeng J Y, Lee E K, Kim B, Kim S and Han K K 2000 *J. Comput. Chem.* **21** 380
[27] Lee Y J, Lee E K, Kim S and Nieminen R M 2001 *Phys. Rev. Lett.* **86** 999
[28] Kang J W and Hwang H J 2001 *Nanotechnology* **12** 295
[29] Michaelian K, Rendon N and Garzon I L 1999 *Phys. Rev.* B **60** 2000
[30] Palacios F J, Iniguez M P, Lopez M J and Alonso J A 1999 *Phys. Rev.* B **60** 2908
[31] Lee R, Pan Z and Ho Y 1996 *Phys. Rev.* B **53** 4156
[32] Li T X, Yin S Y, Ji Y L, Wang B L, Wang G H and Zhao J J 2000 *Phys. Lett.* A **267** 403
[33] Kang J W and Hwang H J 2001 *J. Korean Phys. Soc.* **38** 695
[34] Kang J W and Hwang H J 2002 *Mol. Simul.* **28** 1021
[35] Wang B, Yin S, Wang G and Zhao J 2001 *J. Phys.: Condens. Matter* **13** L403
[36] Kang J W and Hwang H J 2002 *J. Korean Phys. Soc.* **40** 946
[37] Wang B, Wang G and Zhao J 2002 *Phys. Rev.* B **65** 125305
[38] Ding F, Li H J, Wang J, Shen W and Wang G 2002 *J. Phys.: Condens. Matter* **14** 113
[39] Ercolessi F, Parrinello M and Tosatti E 1988 *Phil. Mag.* A **58** 213